were estimated with the Kaplan–Meier method, and the groups were compared using the log–rank test. All results were considered significant at $P < 0.05$. StatMate IV software (ATMS, Tokyo, Japan) was used for all statistical analyses.

RESULTS

Patient characteristics and interventions

MEAN AGE OF the 61 included patients (35 males) was 64.0 ± 10.3 years. Baseline demographics and clinical characteristics are shown in Table 1. Pancreatic cancer was the most common etiology (60.7%), and the site of obstruction was at the duodenum in 93.4% and at the pylorus in 6.6% patients. Twenty-six (42.6%) patients had no oral intake (GOOSS ≤ 0), and 16 patients (26.3%) had a KPS ≤ 50 before stenting.

Table 1 Patient demographics and clinical characteristics ($N = 61$)

Mean age ± SD (years)	64.0 ± 10.3
Sex, *n* (%)	
Male	35 (57.4)
Female	26 (42.6)
Tumor diagnosis, *n* (%)	
Pancreatic cancer	37 (60.7)
Gastric cancer	6 (9.8)
Duodenal cancer	3 (4.9)
Cancer of duodenal papilla	1 (1.6)
Bile duct cancer	9 (14.8)
Gallbladder cancer	2 (3.3)
Metastasis	3 (4.9)
Renal cancer	1 (1.6)
Colon cancer	1 (1.6)
Breast cancer	1 (1.6)
Site of obstruction, *n* (%)	
Pylorus	4 (6.6)
Duodenum, pars I	21 (34.4)
Duodenum, pars II	17 (27.9)
Duodenum, pars III	19 (31.1)
Ability of oral intake (GOOSS)	
Median score, *n* (%) [quartile]	1 [0–1]
0	26 (42.6)
1	25 (41.0)
2	10 (16.4)
Karnofsky performance score	
Median score, *n* (%) [quartile]	60 [60–70]
20–30	2 (3.3)
40–50	14 (23.0)
60–70	39 (63.9)
80	6 (9.8)

GOOSS, gastric outlet obstruction scoring system.
0, no oral intake; 1, liquids only; 2, soft solids; 3, low-residue diet; 4, normal diet.

Clinical outcomes related to stent intervention

Clinical results

Additional stent interventions were required in 14 of 61 cases (11 second stents and 3 third stents). There was no difference in median procedure time between the first stent interventions (First-stent group) and the additional stent interventions (Add-stent group) (21 *vs* 22 min, $P = 0.72$) (Table 2), with 100% technical success rates in both. Median post-procedure length of hospitalization was also similar: 11 days for the First-stent group, and 10 days for the Add-stent group ($P = 0.43$).

Median time to oral fluid intake and oral solids intake was 1 day and 2 days, respectively, in both groups ($P = 0.27$, and 0.09, respectively). Median maximum GOOSS after intervention was 3 ($P = 0.87$), and median recovered GOOSS was 2 in both groups ($P = 0.12$). Clinical effect at 1 week was good, moderate, and poor in 83.6%, 6.6%, and 9.8% in the First-stent group, and 85.7%, 0%, and 14.3% in the Add-stent group, respectively. Median stent patency was 230 days in the First-stent group and 172 days in the Add-stent group ($P = 0.47$) (Fig. 1).

Stent dysfunction and complications

Causes of 15 episodes of initial stent dysfunction were tumor ingrowth in seven, tumor overgrowth in six, and stent migration in two patients. Causes of five repeat stent dysfunctions were tumor ingrowth and stent breakage in one patient each, and tumor overgrowth in three patients (Table 3). Early complications, occurring within 1 week of the procedure, and late complications, occurring 1 week after the procedure, are shown in Table 3. In one case, we detected that the stent was spontaneously disrupted by a CT scan 205 days after the previous intervention. In four cases, bilirubin levels increased 1 day after the procedure, suggesting the possibility that the duodenal stent had accelerated the jaundice.

Factors related to poor effectiveness

Gastroduodenal stent intervention was ineffective for resumption of oral intake and/or symptom relief in 12 cases (Table 4). We examined the following factors for any relationship with poor effectiveness: sex, tumor type, site of obstruction, tumor stage, baseline-GOOSS, KPS ≤ 50, additional stenting, previous biliary stenting, ascites, and peritoneal dissemination. Univariate analysis identified KPS ≤ 50 ($P = 0.03$), ascites ($P = 0.009$), and peritoneal dissemination ($P = 0.001$) as significant factors (Table 4). On multivariate logistic regression analysis, peritoneal dissemination was a

Table 2 Clinical feasibility and efficacy of stent interventions

	First-stent group $N = 61$	Add-stent group $N = 14$	*P*-value
Technical success, *n* (%)	61 (100)	14 (100)	NA
Median procedure time, min [quartile]	21 [18–30]	22 [18–33]	0.72
Median time to oral fluids, days [quartile]	1 [1–1]	1 [1–1]	0.27
Median time to oral solids, days [quartile]	2 [1–3]	2 [1–3]	0.09
Median post-procedure length of hospitalization, days [quartile]	11 [7–22]	10 [7–22]	0.43
Post-procedure oral intake ability			
Median maximum GOOSS [quartile]	3 [3–4]	3 [3–4]	0.87
Median recovered GOOSS [quartile]	2 [1–3]	2 [1–3]	0.12
Clinical effect†, *n* (%)			0.7
Good	51 (83.6)	12 (85.7)	
Moderate	4 (6.6)	0 (0)	
Poor	6 (9.8)	2 (14.3)	

†Good: improvement of both oral intake and symptoms 1 week after intervention.
Moderate: improvement of either oral intake or symptoms 1 week after intervention. Poor: improvement of neither oral intake nor symptoms 1 week after intervention.
GOOSS, gastric outlet obstruction scoring system; NA, not applicable.

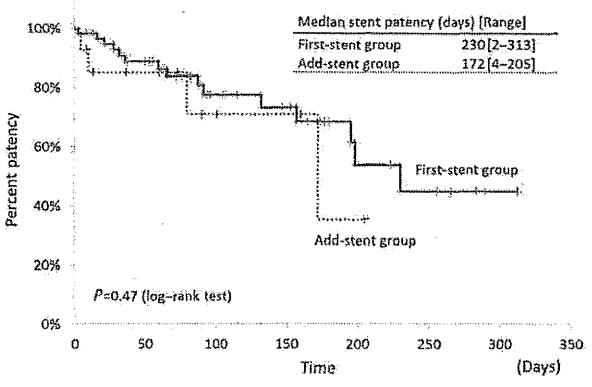

Figure 1 Stent patency is shown with the Kaplan–Meier method. There is no significant difference in median stent patency.

significant independent factor related to poor effectiveness, with an odds ratio of 9.94 (95% confidence interval: 1.82–53.2, $P = 0.01$) (Table 4).

Long-term outcomes of all patients

Long-term outcome was studied in 50 patients with single-stent intervention (First-stent-intervention-only group) and in 11 patients with additional stent intervention (Additional-stent-intervention group). Details of oral intake ability of the patients in the two groups are given in Table 5. Median duration of oral intake, the eating period, was 81 days in the First-stent-intervention-only group and 187 days in the Additional-stent-intervention group, but there was no significant difference ($P = 0.14$). Median survival time after first stent intervention in the Additional-stent-intervention group also tended to be longer than in the First-stent-intervention-only group, but there was no significant difference (First-stent-intervention-only group 94 days *vs* Additional-stent-intervention group 233 days, $P = 0.17$). Most patients could maintain oral intake for a period exceeding half of their remaining lives after first stent intervention (86.0% in the First-stent-intervention-only group and 100% in the Additional-stent-intervention group) (Fig. 2).

Table 3 Stent dysfunction and complications of each stent intervention

	First-stent group $N = 61$	Add-stent group $N = 14$	*P*-value
Stent dysfunction, *n* (%)	15 (24.5)	5 (35.7)	NA
Tumor ingrowth	7	1	
Tumor overgrowth	6	3	
Migration	2	0	
Breakage	0	1	
Early complications, *n* (%)	7 (11.5)	0 (0)	0.18
Stent migration	1	0	
Tumor bleeding	1	0	
Pancreatitis	1	0	
Jaundice	4	0	
Late complications, *n* (%)	7 (11.5)	3 (21.4)	0.32
Stent migration	1	0	
Tumor bleeding	4	0	
Recurrent cholangitis	2	3	

NA, not applicable.

Table 4 Univariate and multivariate analysis of factors related to poor effectiveness in 75 interventions

	Univariate analysis			Multivariate analysis	
	Good $N = 63$	Moderate/poor $N = 12$	*P*-value	Odds ratio	*P*-value
Mean age ± SD, years	63.5 ± 11.0	64.2 ± 10.4	0.53		
Sex					
Male	40	6	0.52		
Female	23	6			
Diagnosis					
Pancreatic cancer	40	4	0.06		
Gastric cancer	6	2			
Duodenal cancer	3	2			
Bile duct cancer	6	4			
Metastasis	3	0			
Other	5	0			
Site of obstruction					
Pylorus	5	2	0.20		
Duodenum, pars I	21	4			
Duodenum, pars II	16	5			
Duodenum, pars III	21	1			
Tumor stage					
Metastatic	41	10	0.32		
Locally advanced	22	2			
Pre-GOOSS ≤0	20	7	0.10		
Karnofsky performance score ≤50	13	6	0.03	1.95	0.39
Additional stent	12	1	0.68		
Billary drainage before intervention	30	6	1.00		
Ascites	14	7	0.009	2.88	0.18
Peritoneal dissemination	16	9	0.001	9.94	0.01

GOOSS, gastric outlet obstruction scoring system.

Thirty patients in the First-stent-intervention-only group were given chemotherapy and three patients (two with pancreatic cancer and one with duodenal cancer) could be resected surgically together with gastroduodenal stents after chemotherapy. In the Additional-stent-intervention group, seven patients were given chemotherapy after the first stenting (Table 5). During their clinical course, 35 patients in the First-stent-intervention-only group (70.0%) and seven patients in the Additional-stent-intervention group (63.6%) required biliary drainage. Methods of biliary drainage are shown in Table 5.

DISCUSSION

FEATURES OF THE Niti-S stent, such as malleable flexibility with a low axial force and a low rate of foreshortening compared with braided-type stents, means the stent can be placed comparatively easily and safely even across angulated strictures, and is also suitable for additional stenting. Clinical data of the Niti-S stent[4,6,7] and other enteral stents are summarized in Table 6. The Wallstent or WallFlex enteral stents (Boston Scientific Japan) were used early and widely in clinical practice before the Niti-S stent became available. Because of the strong axial force of the Wallstent, the risk of kinking and perforation may be increased when used in tortuous and curved anatomy with reported perforation rates of 0–5%. However, these stents have flared ends to reduce the risk of migration which was reported to occur in 0–2% of patients.[12–20]

Dysfunction of uncovered stents would be caused mainly by tumor ingrowth and tumor overgrowth. A recent study reported that a covered metallic stent was associated with less frequent stent dysfunction >4 weeks after stenting, but there was no significant difference in median stent patency.[21] If stent dysfunction occurred, we considered additional stent intervention as a first rescue method based on each patient's condition and prognosis. However, to date, there have been few studies verifying the utility of additional interventions

Table 5 Final ability of oral intake and follow up of all patients after procedure

	Patients with first-stent intervention only $N = 50$	Patients with additional stent intervention $N = 11$	*P*-value
Final ability of oral intake, *n* (%)			0.71
Solids	35 (70.0)	7 (63.6)	
Liquids only	12 (24.0)	4 (36.4)	
NPO	3 (6.0)	0 (0)	
Median eating period (days) [range]	81 [0–313]	187 [31–324]	0.16
Median post-procedure† survival time (days) [range]	94 [8–419]	233 [39–325]	0.17
Percent eating period ≥50%, *n* (%)	43 (86.0)	11 (100)	0.33
Post-procedure† therapy, *n* (%)			1.00
Chemotherapy	31 (62.0)	7 (63.6)	
Surgical resection after chemotherapy	3	0	
Best supportive care	19 (38.0)	4 (36.4)	
Biliary drainage treatments, *n* (%)	35 (70.0)	7 (63.6)	0.73
EBD	24	2	
EUS-BD	5	3	
PTBD	6	2	

†After first intervention.
EBD, endoscopic biliary drainage; EUS-BD, endoscopic ultrasound-guided biliary drainage; GOOSS, gastric outlet obstruction scoring system; NPO, nothing per oral; PTBD, percutaneous transhepatic biliary drainage.

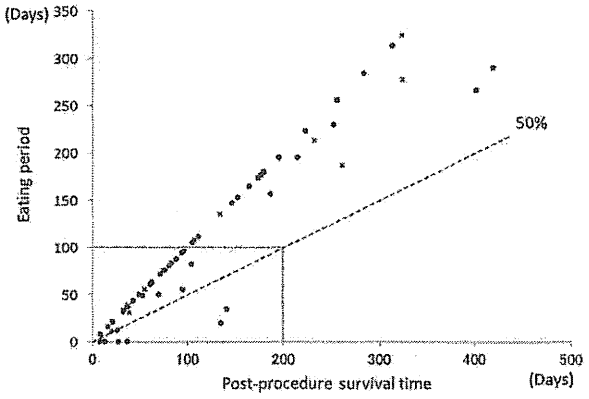

Figure 2 Scatter plot showing eating periods of all patients. Most patients could maintain oral intake for a period exceeding half of their remaining lives after first stent intervention (86.0% in the First-stent-intervention-only group (•) and 100% in the Additional-stent-intervention group (×).

for stent dysfunction.[10] Comparing first stent intervention and additional stent intervention in the present study, clinical feasibility and efficacy were similar with respect to technical success, procedure time, time to oral intake, post-procedure length of hospitalization, improvement of GOOSS, and clinical effect. Technical success and clinical success rates of additional stent intervention were 100% and 85.7%, respectively, which compare favorably with previous reported rates of technical success ranging from 92.9% to 100%, and clinical success ranging from 76.9% to 94.4% (Table 6).[4,6,7,12–20] Overall complication rates are also similar to those from previous studies (from 4% to 36.6%). In the current study, there is no unique complication related to additional stent intervention, which demonstrates the feasibility and safety of additional stent interventions.

We identified the following three features predictive of a suboptimal response to gastroduodenal stenting: KPS ≤ 50, ascites, and peritoneal dissemination. Despite excluding patients with evident distal obstruction of the intestinal tract, presence of peritoneal dissemination was associated with poor clinical effectiveness of gastroduodenal stents. This result was a little different from a previous study which did not find peritoneal dissemination as a negative predictive factor for solid food intake.[22] Although these factors could predict poor effectiveness, we experienced clinical success in more than half of cases even when these factors were present. Hence, in clinical practice, the mere presence of these factors should not be excluded from palliative stenting.[17]

Data from previous studies suggest that bypass surgery should be considered for patients in whom long-term survival >2 months is expected.[8,9] However, recent data also show positive outcomes after stent placement for patients with long survival (Table 6). Hence, the relative indications

Table 6 Comparison of published gastroduodenal stent studies

Study First author	Year	Stent type	No. patients	Technical success *n* (%)	Clinical success *n* (%)	Median eating period (days) [range]	Median survival (days) [range]	Overall complications *n* (%)
Telford *et al.*[12]	2004	Wallstent	176	173 (98.3)	133/159[¶] [83.6]	146[††] [65–202][†]	97 [62–116][†]	14 (8.0)
Graber *et al.*[13]	2007	Wallstent	51	50 (98.0)	43 (84.3)	NR	71.5 [9–515]	17 (33.3)
Maetani *et al.*[6]	2007	Niti-S	37	36 (97.3)	34 (91.9)	NR	118 (NR)	6 (16.2)
van Hooft *et al.*[14]	2009	WallFlex	51	50 (98.0)	43 (84.3)	307[††] [135–470][†]	62 [35–156][‡]	7 (13.7)
Piesman *et al.*[15]	2009	WallFlex	43	41 (95.3)	NR (75)[‡‡]	NR	49 (NR)	15 (34.9)
Shaw *et al.*[16]	2010	WallFlex	70	65 (92.9)	62 (88.6)	NR	54 [3–570]	6 (8.6)
Maetani *et al.*[4]	2010	Niti-S	53	52 (98.1)	50 (94.3)	NR	88 (NR)	13 (24.5)
Mendelsohn *et al.*[17]	2011	WallFlex or Wallstent	201	192 (95.5)	158 (82.3)	NR	160[§§] [10–1312]	NR (4)
Lee *et al.*[18]	2011	Wallstent	57	57 (100)	52 (91.2)	NR	95 [3–1026]	NR[¶¶]
van Hooft *et al.*[7]	2011	Niti-S	52	50 (96.2)	40 (76.9)	43 [190][§]	82 [31–135][‡]	12 (23.1)
Costamagna *et al.*[19]	2012	WallFlex	206	202 (98.1)	NR (91)	NR	94 [79–112][†]	41 (19.9)
Cha *et al.*[20]	2013	Niti-S, UltraFlex or WallFlex	85	82 (96.5)	68 (80.0)	76.1[a] [18–293]	77.3[a] (NR)	NR
Sasaki *et al.*[5]	2013	WallFlex	42	42 (100)	35 (83.3)	90 [33–129][†]	99 [54–180][†]	11 (26.2)
Present study	2014	Niti-S (first stenting)	61	61 (100)	51 (83.6)	81[b] [0–313]	94[b] [8–419]	14 (23.0)
		Niti-S (additional stenting)	14	14 (100)	12 (85.7)	187[c] [31–324]	233[c] [39–325]	3 (21.4)

[†][95% confidence interval].
[‡][quartile].
[§][maximum no. days].
[¶]Seventeen patients were excluded from the analysis after stent insertion.
[††]Data were calculated from only the patient population who could attain clinical success.
[‡‡]Percentage of patients who attained a GOOSS increase ≥1 seven days after procedure.
[§§]Data were calculated from patients with carcinomatosis.
[¶¶]Publication does not state whether the events occurred with duodenal or colonic stents.
[a]Data are mean no. days.
[b]Data are from patients in the First-stent-intervention-only group.
[c]Data are from patients in the Additional-stent-intervention group.
GOOSS, gastric outlet obstruction scoring system; NR, not reported.
Niti-S stent, Taewoong Medical, Seoul, Korea; UltraFlex stent, Boston Scientific Japan, Tokyo, Japan; WallFlex stent, Boston Scientific Japan; Wallstent, Boston Scientific Japan.

of stenting and surgical bypass need to be redefined. We had patients who achieved long-term survival after first stent intervention and who continued therapy for their malignancy with additional stent interventions. Our data show the median eating period after first stenting was 81 days in the patients with a first stent only, and 187 days in the patients with additional stenting; the median overall survival time in the present patient population was 94 days and 233 days, respectively. The present results of first-stent patents were similar to those from recent studies, whereas additional-stent patients showed relatively longer outcomes than recent studies (Table 6). The good outcomes achieved with additional stenting to maintain patency of the gastric outlet confirm the utility of gastroduodenal stenting among

patients with predicted long survival. As a result, most patients could be given chemotherapy soon after the first procedure because of its lesser invasiveness and safety, which is a substantial advantage over bypass surgery. Moreover, some patients with a good response to chemotherapy underwent surgical resection of their original tumor, which indicates the utility of gastroduodenal stenting for patients with GOO who will undergo neoadjuvant chemotherapy as a 'bridge to surgery'.

Forty-two patients required biliary drainage, of which 34 patients were successfully treated with endoscopic techniques, including endoscopic ultrasound-guided biliary drainage (EUS-BD). There have been only a few studies to determine the feasibility of combined endoscopic biliary and gastroduodenal stenting,[23,24] and it remains controversial which biliary drainage method should be selected.

There are some unique points in our study. Although this study enrolled only patients without prior surgical resection of the stomach or duodenum who were treated with the Niti-S stent only, more than 60 patients and 70 interventions could be evaluated. Previous studies included patients who had obstruction of surgical anastomoses and efferent loops, and had been treated with various types of stent.[4,6,7,12–20] Moreover, we estimated the feasibility and efficacy of additional stent interventions by the comparison between first and additional stent interventions. Therefore, the present study is the first to have accurately evaluated the efficacy of the Niti-S stent for gastroduodenal outlet patency, additional interventions, and factors related to poor effectiveness. All stent interventions were carried out at each center under the supervision of experienced endoscopists; therefore, the data may not be generalized to other patient populations. However, the technical success rate was 100%.

In conclusion, despite the presence of factors related to poor effectiveness, endoscopic gastroduodenal stenting would be the first treatment of choice for GOO without multiple levels of obstruction as it provides long-term benefits independently of patient prognosis. If stent dysfunction occurs, additional stent intervention would enable safe continued oral intake, and more patients could obtain long-term benefits.

CONFLICT OF INTERESTS

AUTHORS DECLARE NO conflict of interests for this article.

REFERENCES

1 Yim HB, Jacobson BC, Saltzman JR *et al.* Clinical outcome of the use of enteral stents for palliation of patients with malignant upper GI obstruction. *Gastrointest. Endosc.* 2001; **53**: 329–32.
2 Wong YT, Brams DM, Munson L *et al.* Gastric outlet obstruction secondary to pancreatic cancer: Surgical vs endoscopic palliation. *Surg. Endosc.* 2002; **16**: 310–12.
3 Chandrasegaram MD, Eslick GD, Mansfield CO *et al.* Endoscopic stenting versus operative gastrojejunostomy for malignant gastric outlet obstruction. *Surg. Endosc.* 2012; **26**: 323–9.
4 Maetani I, Ukita T, Nambu T *et al.* Comparison of UltraFlex and Niti-S stents for palliation of unresectable malignant gastroduodenal obstruction. *Dig. Endosc.* 2010; **22**: 83–9.
5 Sasaki T, Isayama H, Maetani I *et al.* Japanese multicenter estimation of WallFlex duodenal stent for unresectable malignant gastric outlet obstruction. *Dig. Endosc.* 2013; **25**: 1–6.
6 Maetani I, Isayama H, Mizumoto Y. Palliation in patients with malignant gastric outlet obstruction with a newly designed enteral stent: A multicenter study. *Gastrointest. Endosc.* 2007; **66**: 355–60.
7 van Hooft JE, van Montfoort ML, Jeurnink SM *et al.* Safety and efficacy of a new non-foreshortening nitinol stent in malignant gastric outlet obstruction (DUONITI study): A prospective, multicenter study. *Endoscopy* 2011; **43**: 671–5.
8 Jeurnink SM, van Eijck CH, Steyerberg EW, Kuipers EJ, Siersema PD. Stent versus gastrojejunostomy for the palliation of gastric outlet obstruction: A systematic review. *BMC Gastroenterol.* 2007; **7**: 18.
9 Jeurnink SM, Steyerberg EW, van Hooft JE *et al.* Surgical gastrojejunostomy or endoscopic stent placement for the palliation of malignant gastric outlet obstruction (SUSTENT study): A multicenter randomized trial. *Gastrointest. Endosc.* 2010; **71**: 490–9.
10 Kang MK, Song HY, Kim JW *et al.* Additional gastroduodenal stent placement: Retrospective evaluation of 68 consecutive patients with malignant gastroduodenal obstruction. *Acta Radiol.* 2013; **54**: 944–8.
11 Adler DG, Baron TH. Endoscopic palliation of malignant gastric outlet obstruction using self-expanding metal stents: Experience in 36 patients. *Am. J. Gastroenterol.* 2002; **97**: 72–8.
12 Telford JJ, Carr-Locke DL, Baron TH *et al.* Palliation of patients with malignant gastric outlet obstruction with the enteral Wallstent: Outcomes from a multicenter study. *Gastrointest. Endosc.* 2004; **60**: 916–20.
13 Graber I, Dumas R, Filoche B *et al.* The efficacy and safety of duodenal stenting: A prospective multicenter study. *Endoscopy* 2007; **39**: 784–7.
14 van Hooft JE, Uitdehaag MJ, Bruno MJ *et al.* Efficacy and safety of the new WallFlex enteral stent in palliative treatment of malignant gastric outlet obstruction (DUOFLEX study): A prospective multicenter study. *Gastrointest. Endosc.* 2009; **69**: 1059–66.
15 Piesman M, Kozarek RA, Brandabur JJ *et al.* Improved oral intake after palliative duodenal stenting for malignant obstruction: A prospective multicenter clinical trial. *Am. J. Gastroenterol.* 2009; **104**: 2404–11.

16 Shaw JM, Bornman PC, Krige JE, Stupart DA, Panieri E. Self-expanding metal stents as an alternative to surgical bypass for malignant gastric outlet obstruction. *Br. J. Surg.* 2010; **97**: 872–6.
17 Mendelsohn RB, Gerdes H, Markowitz AJ, DiMaio CJ, Schattner MA. Carcinomatosis is not a contraindication to enteral stenting in selected patients with malignant gastric outlet obstruction. *Gastrointest. Endosc.* 2011; **73**: 1135–40.
18 Lee EY, Bourke MJ, Williams SJ *et al.* Severity of initial stent angulation predicts reintervention after successful palliative enteral stenting for malignant luminal obstruction. *J. Gastroenterol. Hepatol.* 2011; **26**: 484–91.
19 Costamagna G, Tringali A, Spicak J *et al.* Treatment of malignant gastroduodenal obstruction with a nitinol self-expanding metal stent: An international prospective multicentre registry. *Dig. Liver Dis.* 2012; **44**: 37–43.
20 Cha BH, Lee SH, Kim JE *et al.* Endoscopic self-expandable metallic stent placement in malignant pyloric or duodenal obstruction: Does chemotherapy affect stent patency? *Asia Pac. J. Clin. Oncol.* 2013; **9**: 162–8.
21 Maetani I, Mizumoto Y, Shigoka H *et al.* Placement of a triple-layered covered versus uncovered metallic stent for palliation of malignant gastric outlet obstruction: A multicenter randomized trial. *Dig. Endosc.* 2014; **26**: 192–99.
22 Sasaki T, Isayama H, Nakai Y *et al.* Predictive factors of solid food intake in patients with malignant gastric outlet obstruction receiving self-expandable metallic stents for palliation. *Dig. Endosc.* 2012; **24**: 226–30.
23 Kim KO, Kim TN, Lee HC. Effectiveness of combined biliary and duodenal stenting in patients with malignant biliary and duodenal obstruction. *Scand. J. Gastroenterol.* 2012; **47**: 962–7.
24 Mutignani M, Tringali A, Shah SG *et al.* Combined endoscopic stent insertion in malignant biliary and duodenal obstruction. *Endoscopy* 2007; **39**: 440–7.

J Gastroenterol
DOI 10.1007/s00535-014-0987-2

The Japanese Society of Gastroenterology

ORIGINAL ARTICLE—LIVER, PANCREAS, AND BILIARY TRACT

Does the WHO 2010 classification of pancreatic neuroendocrine neoplasms accurately characterize pancreatic neuroendocrine carcinomas?

Susumu Hijioka · Waki Hosoda · Nobumasa Mizuno · Kazuo Hara · Hiroshi Imaoka · Vikram Bhatia · Mohamed A. Mekky · Masahiro Tajika · Tsutomu Tanaka · Makoto Ishihara · Tatsuji Yogi · Hideharu Tsutumi · Toshihisa Fujiyoshi · Takamitsu Sato · Nobuhiro Hieda · Tsukasa Yoshida · Nozomi Okuno · Yasuhiro Shimizu · Yasushi Yatabe · Yasumasa Niwa · Kenji Yamao

Received: 21 May 2014 / Accepted: 31 July 2014

Abstract
Background The WHO classified pancreatic neuroendocrine neoplasms in 2010 as G1, G2, and neuroendocrine carcinoma (NEC), according to the Ki67 labeling index (LI). However, the clinical behavior of NEC is still not fully studied. We aimed to clarify the clinicopathological and molecular characteristics of NECs.
Methods We retrospectively evaluated the clinicopathological characteristics, *KRAS* mutation status, treatment response, and the overall survival of eleven pNEC patients diagnosed between 2001 and 2014 according to the WHO 2010. We subclassified WHO-NECs into well-differentiated NEC (WDNEC) and poorly differentiated NEC (PDNEC). The latter was further subdivided into large-cell and small-cell subtypes.
Results The median Ki67 LI was 69.1 % (range 40–95 %). Eleven WHO-NECs were subclassified into 4 WDNECs and 7 PDNECs. The latter was further separated into 3 large-cell and 4 small-cell subtypes. Comparisons of WDNEC vs. PDNEC revealed the following traits: hypervascularity on CT, 50 % (2/4) vs. 0 % (0/7) ($P = 0.109$); median Ki67 LI, 46.3 % (40–53 %) vs. 85 % (54–95 %) ($P = 0.001$); Rb immunopositivity, 100 % (4/4) vs. 14 % (1/7) ($P = 0.015$); *KRAS* mutations, 0 % (0/4) vs. 86 % (6/7) ($P = 0.015$); response rates to platinum-based chemotherapy, 0 % (0/2) vs. 100 % (4/4) ($P = 0.067$), and median survival, 227 vs. 186 days ($P = 0.227$).
Conclusions The WHO-NEC category may be composed of heterogeneous disease entities, namely WDNEC and PDNEC. These subgroups tended to exhibit differing profiles of Ki67 LI, Rb immunopositivity and *KRAS* mutation, and distinct response to chemotherapy. Further studies for the reevaluation of the current WHO 2010 classification are warranted.

Keywords Neuroendocrine carcinoma · Ki67 labeling index · *KRAS* mutation · WHO classification

Abbreviations

NEN	Neuroendocrine neoplasm
WHO	World Health Organization

S. Hijioka and W. Hosoda contributed equally to this work.

Electronic supplementary material The online version of this article (doi:10.1007/s00535-014-0987-2) contains supplementary material, which is available to authorized users.

S. Hijioka (✉) · N. Mizuno · K. Hara · H. Imaoka · T. Yogi · H. Tsutumi · T. Fujiyoshi · T. Sato · N. Hieda · T. Yoshida · N. Okuno · K. Yamao
Department of Gastroenterology, Aichi Cancer Center Hospital, 1-1 Kanokoden, Chikusa-ku, Nagoya 464-8681, Japan
e-mail: rizasusu@aichi-cc.jp

W. Hosoda · Y. Yatabe
Department of Pathology and Molecular Diagnostics, Aichi Cancer Center Hospital, Nagoya, Japan

V. Bhatia
Department of Medical Hepatology, Institute of Liver and Biliary Sciences, Delhi, India

M. A. Mekky
Department of Tropical Medicine and Gastroenterology, Assiut University Hospital, Assiut, Egypt

M. Tajika · T. Tanaka · M. Ishihara · Y. Niwa
Department of Endoscopy, Aichi Cancer Center Hospital, Nagoya, Japan

Y. Shimizu
Department of Surgery, Aichi Cancer Center Hospital, Nagoya, Japan

Published online: 21 August 2014

NET	Neuroendocrine tumor
NEC	Neuroendocrine carcinoma
EUS-FNA	Endoscopic ultrasound-guided fine needle aspiration
ENETS	European Neuroendocrine Tumor Society
IHC	Immunohistochemistry
PCR	Polymerase chain reaction
SD	Standard deviation
LCNEC	Large-cell NEC
SCNEC	Small cell-NEC
PDAC	Pancreatic ductal adenocarcinoma

Introduction

Ki67 is a powerful prognostic marker of pancreatic neuroendocrine neoplasms (pNENs) [1] and, accordingly, the remarkable revision was made from the former 2000 World Health Organization (WHO) classification system to the current WHO 2010 terminology system, in which mitotic count and/or Ki67 labeling index (LI) were adopted as the pivotal indicator of stratification [2]. NENs are now to be categorized into neuroendocrine tumor (NET)-G1, NET-G2, and neuroendocrine carcinoma (NEC). Whereas NETs-G1/G2 are invariably composed of tumor cells with well-differentiated morphology, NECs usually have poorly differentiated histology with Ki67 LI > 20 % [2, 3]. Accordingly, all NENs with Ki67 LI > 20 % are defined as NEC. Clinically, these tumors are treated with the same platinum-based chemotherapy regimens as small-cell lung cancers [4–6]. However, some reports have recently indicated that a proportion of well-differentiated NENs might have proliferative rates above the threshold for NET-G2 [7, 8]. In addition, the Nordic NEC study reported that patients with a Ki67 <55 % had low responses to platinum-based chemotherapy [9]. We suppose that the current NEC category, as defined by the WHO 2010 classification (WHO-NEC), includes two groups that differ in clinical behaviors as well as pathological characteristics. Information about the clinicopathological features of WHO-NEC group is scant [7–10]. Therefore, we aimed to further characterize the WHO-NEC group in terms of pathological findings, molecular characteristics, and clinical behaviors.

Patients and methods

Patients

We retrospectively retrieved all of the pNENs diagnosed between January 2001 and March 2014 from our hospital database. All patients were recategorized as NET-G1, NET-G2, or NEC according to the WHO 2010 classification. Specimens for histological examination were obtained from preoperative endoscopic ultrasound-guided fine needle aspiration (EUS-FNA), biopsy, and/or surgical resection. All patients diagnosed with small-cell carcinoma were subsequently assessed by contrast enhanced (CE) chest MDCT to exclude the possibility of metastasis from a primary lung cancer [11]. This study was approved by our institutional review board.

Diagnostic and prognostic characterization

The following features were recorded for all patients: age, gender, symptoms, hormonal syndromes, primary and metastatic locations, European Neuroendocrine Tumor Society (ENETS) TNM stage [12], and CE-MDCT features such as anatomical location, tumor size, and contrast enhancement. We recorded the details of all treatments administered to the patients, particularly platinum-based chemotherapy [4, 5, 13].

Endoscopic ultrasound-guided fine needle aspiration (EUS-FNA) and sample preparation

EUS-FNA procedures were performed using a convex linear-array echoendoscope (GF-UGT240 or GF-UCT260; Olympus Optical Co Ltd, Tokyo, Japan) paired with an ultrasound machine (SSD5500 or Prosound α10; Aloka, Tokyo, Japan). We used 22-gauge needles (NA-11J-KBor NA-200H-8022; Olympus Medical System Corp. Ltd., Tokyo, Japan or EchoTip-Ultra Needle; Cook Endoscopy Inc., Winston Salem, N.C., USA or Expect; Boston Scientific Japan, Tokyo, Japan).

Aspirated materials were divided for cytopathological evaluation, cell-block preparation, and *KRAS* mutation analysis. In all patients, specimen adequacy was evaluated on-site by Diff Quick staining (Diff-Quik; Kokusai Shiyaku, Kobe, Japan) by a cytopathologist or cytotechnologist. Cell-blocks were prepared after the fresh specimens were immediately fixed in 10 % formalin and embedded in paraffin. Sliced sections then were stained by hematoxylin and eosin, as well as by immunohistochemical staining (IHC) [14].

Histological evaluation

We defined tumors as NEC that showed diffuse expression of neuroendocrine markers and Ki67 LI of more than 20 %. In accordance with the 2010 WHO classification, tumors characterized by high-grade cytological atypia, apparent pleomorphism, extensive necrosis, and prominent mitotic activity were categorized into poorly differentiated NEC

(PDNEC). Of PDNECs, tumors characterized by diffuse growth of highly atypical cells with small-sized to medium-sized nuclei, finely granular chromatin, and inconspicuous nucleoli, were categorized as small-cell NEC (SCNEC). Carcinomas with large nuclei, coarse chromatin and well-visible nucleoli with nested proliferation were categorized as large-cell NEC (LCNEC). Furthermore, we attempted to extract those tumors whose cytological features were blander than that of PDNEC and rather similar to NET-G2; that is, tumors composed predominantly of cells with low nucleocytoplasmic ratio and small-sized to medium-sized, ovoid nuclei, growing with minimal pleomorphism, and lacking extensive necrosis. We designated these tumors as 'well differentiated NEC (WDNEC)', and separated them from SCNECs and LCNECs. All slides were reviewed and reclassified by the same pathologist (WH).

Immunohistochemistry and Ki67 labeling index

IHC was performed using monoclonal antibodies for chromogranin A (clone SP12, rabbit, 1:200, Neo Markers), synaptophysin (clone SP11, rabbit, 1:100, Neo Markers, Fremont, CA, USA), Ki67 (clone SP6, rabbit, 1:200; Neo Markers), and Rb (clone 3H9, mouse, 1:300; MBL).

The measurement of Ki67 LI was performed under the assistance of digital pathology technology. Briefly, slides were digitally scanned using a Scan Scope XT (Aperio Technologies, Vista, CA, USA). All sections were reviewed to exclude portions with extensive desmoplasia, necrosis and regions with bleeding. The ultimate Ki67 LI was determined as the highest value found in each specimen using the IHC Nuclear Image Analysis tool (Aperio Technologies, Vista, CA, USA) and was similarly measured and determined in cell-block sections of EUS-FNA specimens as described previously [15].

The prominent concern about EUS-FNA is whether WHO classification (grading) is possible with the biopsy specimens. We previously reported a study [15] about a comparison of grades of pNENs between resected and EUS-FNA specimens by Ki67 immunostaining. The concordance rate rose to 90 % when EUS-FNA samples contained more than 2000 neoplastic cells. In accordance with our previous study, we defined the cases whose neoplastic cells were insufficient for grading (less than 2000 cells) as tumors of 'uncertain' grade.

Analysis of KRAS mutation

Genetic analysis was performed on either the fresh specimens or formalin-fixed paraffin-embedded sections. After nucleic acids were extracted and amplified by polymerase chain reaction, gene mutations were analyzed by ABI PRISM 310 Genetic Analyzer (Applied Biosystems) or the Cycleave PCR assay (Takara Co., Ltd); the detail of which was described previously [16, 17].

Statistical analysis

Statistical analysis was performed using SPSS 17.0 (SPSS Inc., Chicago, IL, USA) software and P values <0.05 were considered statistically significant. Categorical variables are expressed as absolute (n) and relative (%) frequencies and were compared using the Chi squared test or Fisher's exact test. Survival was analyzed using the Kaplan–Meier method with the log-rank test.

Results

Ninety-five patients were diagnosed with pNEN at our hospital during the study period. As to grading of pNENs, the WHO classification 2010 suggests two parameters (mitotic count and Ki67 LI) to evaluate the proliferative activity of tumors. We performed grading of pNENs by measuring Ki67 LI and did not employ the mitotic count method, because our study consisted mostly of tumors diagnosed by FNA specimens, which were too small an amount to secure 50 microscopic fields necessary for the calculation of mitotic count. The pNENs were reclassified into uncertain for Ki67 LI ($n = 8$), NET-G1 ($n = 55$), NET-G2 ($n = 21$), and WHO-NEC ($n = 11$) in accordance with the WHO 2010 classification. The 11 cases of WHO-NEC were the subject of analysis in this study (Fig. 1).

Basic demographic and clinical features of patients with WHO-NEC (Tables 1, 2)

Ten (91 %) of 11 patients were symptomatic, mainly with abdominal pain. The median tumor size was 35 mm (range 20–55 mm). Tumors were located in the head, body, and tail of the pancreas in 2, 5, and 4 patients, respectively. Eight (72 %) patients had liver metastasis at the time of diagnosis, two were treated with surgery (ENETS stageIIb and IIIb) and six who received platinum-based chemotherapy (3 cases were cisplatin + irinotecan and 3 cases were cisplatin + etoposide) had a response rate of 67 %. In the remaining 2 patients, one patient received Gemcitabine (case 3) and another patient received Everolimus because we defined it as WDNEC (case 9). The overall median survival was 314 days (range 60–1202 days).

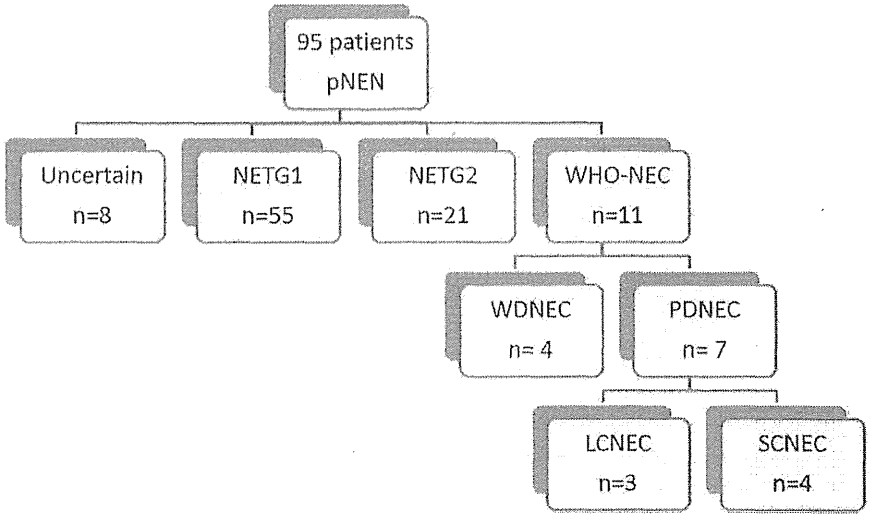

Fig. 1 Algorithm for patient selection from pNEN. *NEN* neuroendocrine neoplasm, *NET* neuroendocrine tumor, *LCNEC* large cell NEC, *SCNEC* small cell NEC, *WDNEC* well-differentiated neuroendocrine carcinoma, *PDNEC* poorly-differentiated neuroendocrine carcinoma

Table 1 Patient characteristics ($n = 11$)

Gender	
Male/female	6/5
Age	
Median (range)	59 years (28–74)
Symptom	
Yes (%)	91 % (abdominal pain)
Site of pancreas tumor	
Head/body/tail	2/5/4
Tumor size	
Median (range)	35 mm (20–55)
Metastasis	
Yes (%)	72 % (liver metastasis)
Treatment	
Operation/chemotherapy/BSC	2/8/1

Imaging features of WHO-NEC on CE-MDCT (Fig. 2; Supplementary Table)

Assessment by CE-MDCT revealed that 9 (82 %) of 11 WHO-NEC in the pancreas were hypovascular. Eight of these tumors had metastasized to the liver, where 7 (88 %) of them were also hypovascular, like the primary tumor (Fig. 2). Before biopsy confirmation, NEN were suspected in only two patients, and the imaging features in the remaining 9 (82 %), suggested pancreatic ductal adenocarcinoma (PDAC). The main pancreatic duct was dilated in 4 (57 %) of 7 patients with tumors located in the head and body of the pancreas.

Pathological and molecular characteristics of WHO-NEC (Fig. 3, Supplementary Figure; Tables 2, 3)

A total of 11 WHO-NEC cases were submitted to the pathological and molecular analysis. No ductal carcinoma components were noted. All cases showed diffuse and strong immunoreactivity for neuroendocrine markers except 1 case, in which only synaptophysin was positive. In total, chromogranin A was expressed in 91 % and synaptophysin was expressed in 100 % of cases. The median Ki67 LI was 69.1 % (range 40–95 %). Nuclear expression of Rb protein was retained in 5 (45 %) tumors. *KRAS* mutations were detected in 6 (55 %) tumors. Seven (64 %) and 4 (36 %) of 11 tumors were categorized as PDNEC (4 SCNECs and 3 LCNECs) and WDNEC, respectively, according to their morphologic characteristics that we mentioned in the "Patients and methods" (Fig. 3, Supplementary Figure).

Clinicopathological comparison of well-differentiated and poorly differentiated NEC (Table 4)

The clinicopathological comparison between the WDNEC and PDNEC groups revealed that they were clinically and molecularly different in several aspects as follows: hypervascularity in MDCT images, 50 % (2/4) vs. 0 % (0/7), $P = 0.109$; median Ki67 LI, 46 % (range 40–53 %) vs. 85 % (range 54–95 %), $P = 0.001$; nuclear expression of Rb, 100 % (4/4) vs. 14 % (1/7), $P = 0.015$; *KRAS* mutations, 0 % (0/4) vs. 86 % (6/7), $P = 0.015$; response rates to platinum-based chemotherapy, 0 % (0/2) vs. 100 % (4/4) $P = 0.067$; and median survival, 227 vs. 186 days, $P = 0.227$.

Table 2 Clinical, pathological features, treatment and response for chemotherapy of WHO-NEC patients

Case	Age/ sex	Location	Size (mm)	ENETS stage	Tissue sampling	Histology	Ki67 LI (%)	CGA	Synaptophysin	Rb	*KRAS*	Treatment	Response for platinum-based regimen
1	30, M	Body	45	IIb	Biopsy and surgical resection	WDNEC	40	Positive	Positive	Positive	WT	Operation	ND
2	59, F	Body	30	IIIb	Biopsy and surgical resection	PDNEC (small cell)	80	Positive	Positive	Positive	MT	Operation	ND
3	49, F	Body	35	IV	Biopsy	PDNEC (large cell)	85	Positive	Positive	Negative	MT	CT (Gemcitabine)	ND
4	68, F	Tail	36	IV	Biopsy	WDNEC	48	Positive	Positive	Positive	WT	CT (IP)	PD
5	63, F	Body	33	IV	Biopsy	PDNEC (large cell)	54	Positive	Positive	Negative	MT	CT (IP)	PR
6	61, M	Body	45	IV	Biopsy	PDNEC (large cell)	90	Positive	Positive	Negative	MT	CT (EP)	PR
7	74, M	Head	20	IV	Biopsy	PDNEC (small cell)	90	Positive	Positive	Negative	WT	BSC	ND
8	37, M	Head	20	IV	Biopsy	PDNEC (small cell)	80	Positive	Positive	Negative	MT	CT (EP)	PR
9	50, F	Tail	35	IV	Biopsy	WDNEC	45	Negative	Positive	Positive	WT	CT (Everolimus)	ND
10	55, M	Tail	30	IV	Biopsy	WDNEC	53	Positive	Positive	Positive	WT	CT (EP)	PD
11	66, M	Tail	70	IV	Biopsy	PDNEC (small cell)	95	Positive	Positive	Negative	MT	CT (IP)	PR

CGA chromogranin A, *WT* wild type, *MT* mutant, *CT* chemotherapy, *IP* cisplatin + irinotecan, *EP* cisplatin + etoposide, *BSC* best supportive care, *ND* not done, *PD* progressive disease, *PR* partial response

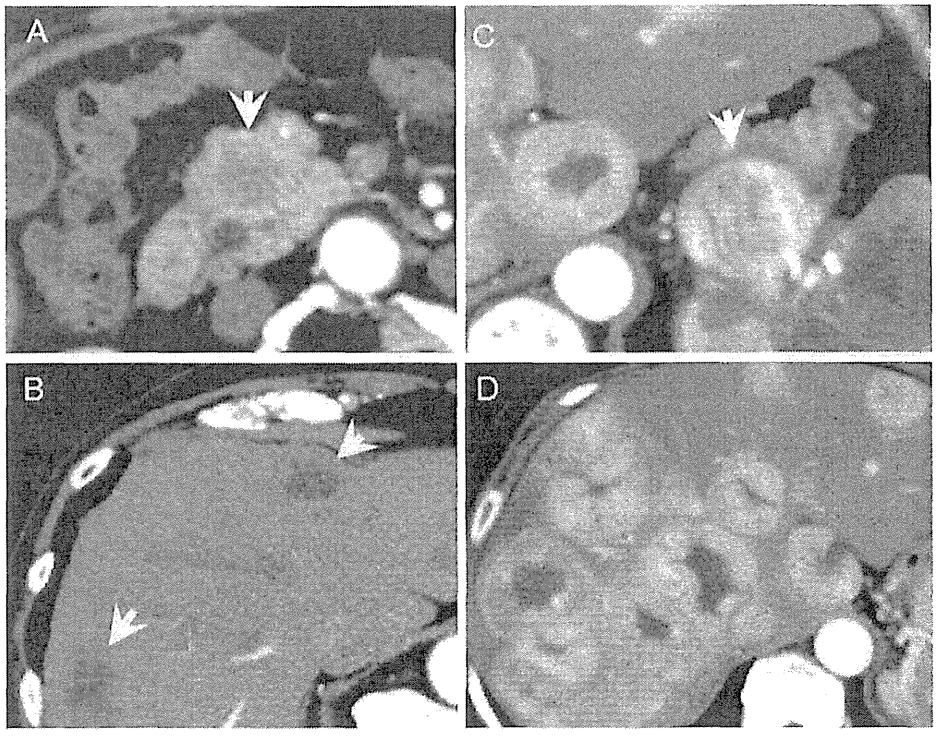

Fig. 2 Computed tomography findings of respective pNECs. **a**, **b** Hypovascular lesions both primary pancreas head site and multiple liver lesions (SCNEC case). **c**, **d** Hypervascular lesions both primary pancreas head site and multiple liver lesions (WDNEC case)

Discussion

When the WHO 2010 classification was applied to our patients with NENs of the pancreas, we found that 36 % of the high-grade category included tumors with well differentiated morphology. This critical finding has an impact on the treatment strategies, particularly the platinum-based chemotherapy which should be originally administered for only PDNEC.

Our findings suggested that WDNECs differ from PDNECs and are rather more closely related to NETs-G2 in terms of clinicopathological and molecular characteristics. Firstly, MDCT consistently showed hypervascularity in WDNEC, but not in PDNEC. Some reports indicated that tumor vascularity correlated with the proliferation index and/or WHO classification [18, 19]. Our findings indicated that only 18 % of WHO-NEC cases were suspected of pNEN according to imaging findings before EUS-FNA, with most being considered PDAC or pancreatic adeno-squamous carcinoma. That is, a significant proportion (82 %) of NECs could not be correctly diagnosed by imaging, especially the PDNEC type.

Histologically, WDNECs shared more morphological traits with NETs-G2 than PDNECs, allowing us to presume that WDNECs correspond to well-differentiated NETs with high proliferative activity. The Ki67 LI tended to be lower in WDNEC than in PDNEC. Notably, *KRAS* and *Rb* genes are promising molecular markers with which to distinguish these types of tumors. The result that *KRAS* mutations were not found in WDNECs supports the notion that this category lies in close proximity to NET-G2, as no pancreatic NETs-G1/G2 have been reported to possess *KRAS* mutations, whereas PDNECs have been shown to harbor *KRAS* mutations [10, 16, 20]. Loss of expression of Rb was found in 86 % of PDNEC cases, whereas all of the WDNEC cases retained its expression. Aberration of the Rb/p16 pathway has been reported to be frequently involved in PDNECs of the pancreas, gallbladder, and ampulla, but not in pancreatic well-differentiated NETs [10, 20–22]. Concerning pancreatic NEN, Yachida et al. [10] conducted immunohistochemical and genetic analyses of several oncogenes and tumor suppressor genes including *KRAS* and *Rb*, and revealed that the aberrations of both genes were common in PDNECs but none in NETs-G1/G2. Their conclusion that PDNECs were molecularly distinct from well-differentiated NETs is in keeping with our findings. Taken together, the difference between WDNEC and PDNEC appears to be clinically, histologically, and molecularly significant, and we consider that WDNECs are more likely to be in the category of well-differentiated NET rather than NEC, thus, favoring the designation, namely "NET-G3".

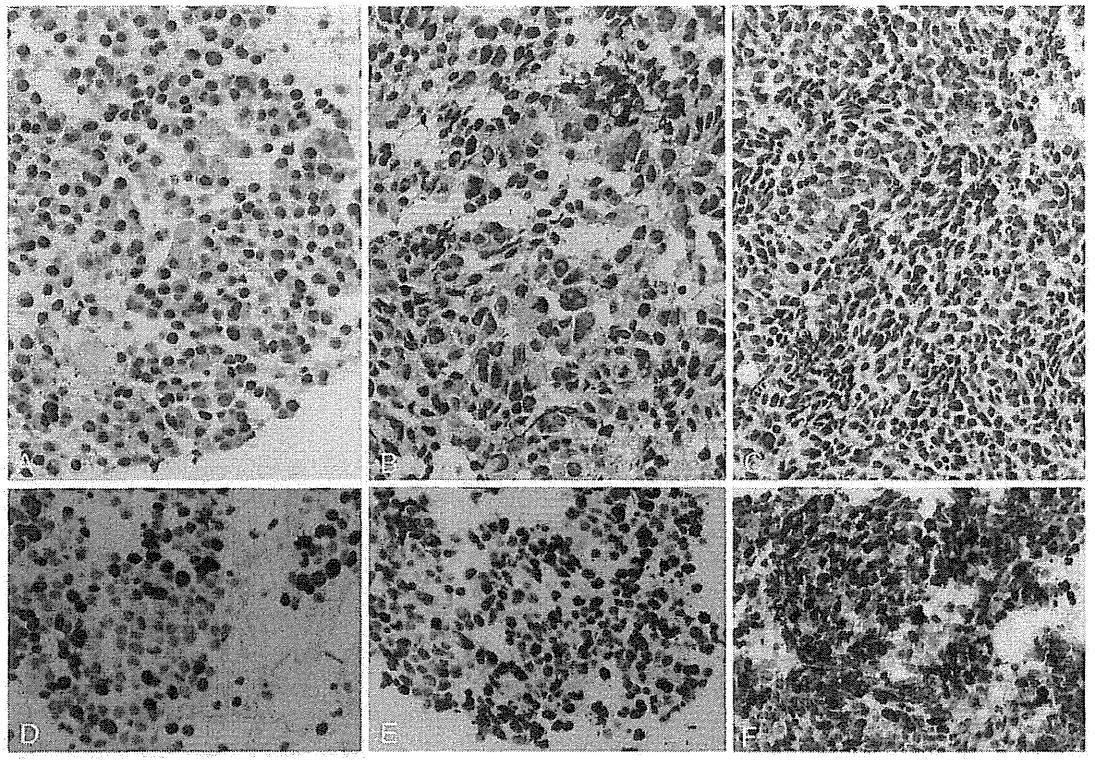

Fig. 3 Histologic features of NECs of the pancreas [H&E stain (**a–c**), and Ki67 (**d–f**), respectively]. The *left column* (**a**, **d**) is a case of WDNEC, the *middle column* (**b**, **e**) is of LCNEC, and the *right column* (**c**, **f**) is of SCNEC. Morphology of WDNECs shows a close similarity to that of NET-G1/G2, characterized by monomorphic growth of tumor cells with highly preserved endocrine cell features. Although LCNECs have features of endocrine cells as well, they are distinguished from WDNECs by increased nuclear atypia, cellular pleomorphism, and the frequent presence of tumor necrosis. SCNECs are composed of small cells with dense chromatin, scarce cytoplasm, and remarkable mitotic activity. These are reminiscent of small cell carcinomas of the lung

Table 3 Pathological and molecular characteristics of WHO-NEC

Ki67 labeling index	
Median (range)	69.1 % (40–95 %)
Morphology	
WDNEC/PDNEC	4/7
Subtypes of PDNEC	
Large-cell type/small-cell type	3/4
Rb immunopositivity	45 % (5/11)
KRAS mutation	54 % (6/11)

WDNEC well-differentiated NEC, *PDNEC* poorly differentiated NEC

Table 4 Clinicopathological comparison of WDNEC and PDNEC

	WDNEC ($n = 4$)	PDNEC ($n = 7$)
Vascularity in pancreas tumor		
Yes (%)	50 % (2/4)	0 % (0/7)
Ki67 labeling index		
Median (range)	46.3 % (40–53 %)	85 % (54–95 %)
Rb immunopositivity	100 % (4/4)	14 % (1/7)
KRAS mutation	0 % (0/4)	86 % (6/7)
Response rate of platinum-based regimen	0 % (0/2)	100 % (4/4)
Prognosis		
Median	227 days	186 days

WDNEC well-differentiated NEC, *PDNEC* poorly differentiated NEC

Our study showed that both WDNEC and PDNEC patients harbored unfavorable outcome (median overall survival of 227 days and 186 days, respectively), which is in stark contrast to NET-G2 patients whose median overall survival is reportedly 162 months [1]. Although WDNEC and PDNEC shared aggressiveness clinically and pathologically, the efficacy of the treatment between them tended to be different; all WDNEC cases did not exhibit response to the platinum-based chemotherapy while all of the PDNEC cases did. The Nordic NEC study [9] found that WHO-NEC with Ki67 LI > 55 % responded to platinum-based chemotherapy, whereas those with Ki67 LI < 55 % did not. Although the Nordic NEC study mainly focused on the treatment and prognostic aspects, there was no detailed description of the pathologic

characteristics of the cases. We suppose that some of their WHO-NEC included WDNEC as defined herein. Based on the results of the Nordic NEC study, the NCCN guidelines noted in footnotes that "intermediate Ki67 levels in the 20–50 % range may not respond well to platinum/etoposide as patients with small cell histology or extremely high Ki67 and so, a clinical judgment should be used". When NEN is diagnosed as WHO-NEC, clinically the toxic platinum-based chemotherapy is usually administered as a first-line regimen. However, a recent case report showed a good response of high-grade NET to molecular targeted therapy with agents such as Everolimus [23]. In fact, one patient who was diagnosed with WDNEC and received Everolimus obtained partial response. The current WHO 2010 classification might be flawed in terms of the management of patients with NEC and the classification scheme for NECs should be revised as the clinical, pathological, and molecular characteristics of this high-grade NEN become more fully clarified.

In regard to IHC, chromogranin A was expressed in 91 % of WHO-NEC cases, and synaptophysin was expressed in 100 %. In a similar fashion, previous articles reported that chromogranin A was expressed in 81–94 %, and synaptophysin was expressed in 88–96 % [7–9]. Taken together, stainability of chromogranin A and synaptophysin is high not only in WDNEC but also in PDNEC.

In our institute, we perform EUS-FNA for the diagnosis of pancreatic tumors on a routine basis, and have been reported its usefulness so far [11, 14–16, 24]. The diagnostic accuracy of overall pancreatic tumors was 91.8 % (918/996) [14]. We previously detected *KRAS* mutations in 87 % (266/307) of EUS-FNA specimens from pancreatic masses in patients with PDAC [24] and none among 25 well-differentiated endocrine tumors [16]. Jiao et al. [20] also reported the absence of *KRAS* mutations in NET-G1/G2.

To the best of our knowledge, this is the first study which examined the clinicopathological characteristics of pNECs, with an emphasis on the difference between WDNEC and PDNEC. However, some limitations should be addressed. The retrospective design hindered precise analysis of all required data, imposed potential selection bias, and the patient cohort was small due to the natural rarity of pNECs that account for <1 % of all pancreatic carcinomas, and 2–7.5 % of all pNEN [2, 25]. Intratumoral heterogeneity is another important consideration. In our 11 cases of NEC, we did not note any adenocarcinoma component histologically nor immunohistochemically. Also, the result of the high frequency of Rb aberration in our series minimizes the possibility of a hidden presence of concomitant adenocarcinomas, as Rb aberration has been reported to be a rare event in PDACs (5–6 %) [26, 27]. Although the above observations do not fully rule out the possibility that some of the cases might contain an accompanying adenocarcinoma, this may be a relatively uncommon occurrence given the low frequency of an associated ductal adenocarcinoma in PDNECs reported by Basturk et al. [8] (6/44, 14 %). Finally, we address the feasibility of grading for pNENs diagnosed by FNA specimens, which constituted most of our series. Past studies of ours and of others claimed that grading by Ki67 LI can be applicable to FNA specimens by showing high concordance between the grade given by the FNA specimens and that by the corresponding resected specimens (concordance rate 78–90 %) [15, 28–31]. Indeed, downgrading or upgrading between G1 and G2 occurred in a small proportion of cases, but there was no tumor observed among the 5 studies that was graded as G3 by EUS-FNA and was downgraded to G2 by surgical resection. This observation, as well as the poor outcome of the current study, indicates that the admixture of 'overestimated' NETs-G2 in our cohort seemed unlikely to happen.

In conclusion, we identified a significant number of "WDNEC" cases among pNECs that were defined by the current WHO classification system. The clinicopathological and molecular analyses suggested that WDNEC is distinct from PDNEC. Though the number of cases we analyzed was limited, we believe that our scheme of subcategorizing pancreatic NEC showed promise. Further larger-scale studies are warranted to validate our stratification of WHO-NECs, which will facilitate a more personalized treatment of the patients with this rare malignant neoplasm.

Acknowledgments This study was supported by a grant from the Pancreas Research Foundation of Japan and JSPS KAKENHI Grant Number 26461041.

Conflict of interest The authors declare that they have no conflict of interest.

References

1. Pape UF, Jann H, Muller-Nordhorn J, et al. Prognostic relevance of a novel TNM classification system for upper gastroenteropancreatic neuroendocrine tumors. Cancer. 2008;113:256–65.
2. Bosman F, Carneiro F, Hruban RH, et al. WHO classification of tumours of the digestive system. Lyon, France: IARC Press; 2010.
3. Rindi G, Klöppel G, Alhman H, et al. TNM staging of foregut (neuro) endocrine tumors: a consensus proposal including a grading system. Virchows Arch. 2006;449:395–401.
4. Moertel CG, Kvols LK, O'Connell MJ, et al. Treatment of neuroendocrine carcinomas with combined etoposide and cisplatin. Evidence of major therapeutic activity in the anaplastic variants of these neoplasms. Cancer. 1991;68:227–32.
5. Mitry E, Baudin E, Ducreux M, et al. Treatment of poorly differentiated neuroendocrine tumours with etoposide and cisplatin. Br J Cancer. 1999;81:1351–5.

6. Pavel M, Baudin E, Couvelard A, et al. ENETS Consensus Guidelines for the management of patients with liver and other distant metastases from neuroendocrine neoplasms of foregut, midgut, hindgut, and unknown primary. Neuroendocrinology. 2012;95:157–76.
7. Velayoudom-Cephise FL, Duvillard P, Foucan L, et al. Are G3 ENETS neuroendocrine neoplasms heterogeneous? Endoc-Relat Cancer. 2013;20:649–57.
8. Basturk O, Tang L, Hruban RH, et al. Poorly differentiated neuroendocrine carcinomas of the pancreas: a clinicopathologic analysis of 44 cases. Am J Surg Pathol. 2014;38:437–47.
9. Sorbye H, Welin S, Langer SW, et al. Predictive and prognostic factors for treatment and survival in 305 patients with advanced gastrointestinal neuroendocrine carcinoma (WHO G3): the NORDIC NEC study. Ann Oncol: Off J Eur Soc Med Oncol/ ESMO. 2013;24:152–60.
10. Yachida S, Vakiani E, White CM, et al. Small cell and large cell neuroendocrine carcinomas of the pancreas are genetically similar and distinct from well-differentiated pancreatic neuroendocrine tumors. Am J Surg Pathol. 2012;36:173–84.
11. Hijioka S, Matsuo K, Mizuno N, et al. Role of endoscopic ultrasound and endoscopic ultrasound-guided fine-needle aspiration in diagnosing metastasis to the pancreas: a tertiary center experience. Pancreatol : Off J Int Assoc Pancreatol. 2011;11: 390–8.
12. Rindi G, Kloppel G, Alhman H, et al. TNM staging of foregut (neuro)endocrine tumors: a consensus proposal including a grading system. Virchows Archiv: Int J Pathol. 2006;449:395–401.
13. Plockinger U, Rindi G, Arnold R, et al. Guidelines for the diagnosis and treatment of neuroendocrine gastrointestinal tumours. A consensus statement on behalf of the European Neuroendocrine Tumour Society (ENETS). Neuroendocrinology. 2004;80:394–424.
14. Haba S, Yamao K, Bhatia V, et al. Diagnostic ability and factors affecting accuracy of endoscopic ultrasound-guided fine needle aspiration for pancreatic solid lesions: Japanese large single center experience. J Gastroenterol. 2013;48:973–81.
15. Hasegawa T, Yamao K, Hijioka S, et al. Evaluation of Ki-67 index in EUS-FNA specimens for the assessment of malignancy risk in pancreatic neuroendocrine tumors. Endoscopy. 2014;46: 32–8.
16. Hosoda W, Takagi T, Mizuno N, et al. Diagnostic approach to pancreatic tumors with the specimens of endoscopic ultrasound-guided fine needle aspiration. Pathol Int. 2010;60:358–64.
17. Yatabe Y, Hida T, Horio Y, et al. A rapid, sensitive assay to detect EGFR mutation in small biopsy specimens from lung cancer. J Mol Diagn. 2006;8:335–41.
18. Rodallec M, Vilgrain V, Couvelard A, et al. Endocrine pancreatic tumours and helical CT: contrast enhancement is correlated with microvascular density, histoprognostic factors and survival. Pancreatol: Off J Int Assoc Pancreatol. 2006;6:77–85.
19. d'Assignies G, Couvelard A, Bahrami S, et al. Pancreatic endocrine tumors: tumor blood flow assessed with perfusion CT reflects angiogenesis and correlates with prognostic factors1. Radiology. 2009;250:407–16.
20. Jiao Y, Shi C, Edil BH, et al. DAXX/ATRX, MEN1, and mTOR pathway genes are frequently altered in pancreatic neuroendocrine tumors. Science. 2011;331:1199–203.
21. Nassar H, Albores-Saavedra J, Klimstra DS. High-grade neuroendocrine carcinoma of the ampulla of vater: a clinicopathologic and immunohistochemical analysis of 14 cases. Am J Surg Pathol. 2005;29:588–94.
22. Parwani AV, Geradts J, Caspers E, et al. Immunohistochemical and genetic analysis of non-small cell and small cell gallbladder carcinoma and their precursor lesions. Mod Pathol: Off J USA Can Acad Pathol Inc. 2003;16:299–308.
23. Fonseca PJ, Uriol E, Galván JA, et al. Prolonged clinical benefit of Everolimus therapy in the management of high-grade pancreatic neuroendocrine carcinoma. Case Rep Oncol. 2013;6: 441–9.
24. Ogura T, Yamao K, Sawaki A, et al. Clinical impact of K-ras mutation analysis in EUS-guided FNA specimens from pancreatic masses. Gastrointest Endosc. 2012;75:769–74.
25. Ito T, Igarashi H, Nakamura K, et al. Epidemiological trends of pancreatic and gastrointestinal neuroendocrine tumors in Japan: a nationwide survey analysis. J Gastroenterol. 2014. doi:10.1007/ s00535-014-0934-2.
26. Barton CM, McKie AB, Hogg A, et al. Abnormalities of the RB1 and DCC tumor suppressor genes: uncommon in human pancreatic adenocarcinoma. Mol Carcinog. 1995;13:61–9.
27. Gerdes B, Ramaswamy A, Ziegler A, et al. p16INK4a is a prognostic marker in resected ductal pancreatic cancer: an analysis of p16INK4a, p53, MDM2, an Rb. Ann Surg. 2002;235:51–9.
28. Weynand B, Borbath I, Bernard V, et al. Pancreatic neuroendocrine tumour grading on endoscopic ultrasound-guided fine needle aspiration: high reproducibility and inter-observer agreement of the Ki-67 labelling index. Cytopathology. 2013. doi:10.1111/ cyt.12111.
29. Piani C, Franchi GM, Cappelletti C, et al. Cytological Ki-67 in pancreatic endocrine tumours: an opportunity for pre-operative grading. Endocr Relat Cancer. 2008;15:175–81.
30. Larghi A, Capurso G, Carnuccio A, et al. Ki-67 grading of nonfunctioning pancreatic neuroendocrine tumors on histologic samples obtained by EUS-guided fine-needle tissue acquisition: a prospective study. Gastrointest Endosc. 2012;76:570–7.
31. Chatzipantelis P, Konstantinou P, Kaklamanos M, et al. The role of cytomorphology and proliferative activity in predicting biologic behavior of pancreatic neuroendocrine tumors: a study by endoscopic ultrasound-guided fine-needle aspiration cytology. Cancer. 2009;117:211–6.

Pancreatology 14 (2014) 221–226

Contents lists available at ScienceDirect

Pancreatology

journal homepage: www.elsevier.com/locate/pan

Original article

Ring-enhancement pattern on contrast-enhanced CT predicts adenosquamous carcinoma of the pancreas: A matched case-control study

Hiroshi Imaoka [a,*], Yasuhiro Shimizu [b], Nobumasa Mizuno [a], Kazuo Hara [a], Susumu Hijioka [a], Masahiro Tajika [a], Tsutomu Tanaka [a], Makoto Ishihara [a], Takeshi Ogura [a], Tomohiko Obayashi [a], Akihide Shinagawa [a], Masafumi Sakaguchi [a], Hidekazu Yamaura [c], Mina Kato [c], Yasumasa Niwa [a], Kenji Yamao [a]

[a] Department of Gastroenterology, Aichi Cancer Center Hospital, Nagoya, Japan
[b] Department of Gastroenterological Surgery, Aichi Cancer Center Hospital, Nagoya, Japan
[c] Department of Diagnostic and Interventional Radiology, Aichi Cancer Center Hospital, Nagoya, Japan

ARTICLE INFO

Article history:
Received 14 August 2013
Received in revised form
2 February 2014
Accepted 16 February 2014
Available online 25 February 2014

Keywords:
Adenosquamous carcinoma of the pancreas (ASC)
Pancreatic ductal adenocarcinoma (PDAC)
Contrast-enhanced computed tomography (CT)
Endoscopic ultrasonography (EUS)
Matched case-control study

ABSTRACT

Objectives: Adenosquamous carcinoma of the pancreas (ASC) is a rare malignant neoplasm of the pancreas, exhibiting both glandular and squamous differentiation. However, little is known about its imaging features. This study examined the imaging features of pancreatic ASC.
Methods: We evaluated images of contrast-enhanced computed tomography (CT) and endoscopic ultrasonography (EUS). As controls, solid pancreatic neoplasms matched in a 2:1 ratio to ASC cases for age, sex and tumor location were also evaluated.
Results: Twenty-three ASC cases were examined, and 46 solid pancreatic neoplasms (43 pancreatic ductal adenocarcinomas, two pancreatic neuroendocrine tumors and one acinar cell carcinoma) were matched as controls. Univariate analysis demonstrated significant differences in the outline and vascularity of tumors on contrast-enhanced CT in the ASC and control groups ($P < 0.001$ and $P < 0.001$, respectively). A smooth outline, cystic changes, and the ring-enhancement pattern on contrast-enhanced CT were seen to have significant predictive powers by stepwise forward logistic regression analysis ($P = 0.044$, $P = 0.010$, and $P = 0.001$, respectively). Of the three, the ring-enhancement pattern was the most useful, and its predictive diagnostic sensitivity, specificity, positive predictive value and negative predictive value for diagnosis of ASC were 65.2%, 89.6%, 75.0% and 84.3%, respectively.
Conclusions: These results demonstrate that presence of the ring-enhancement pattern on contrast-enhanced CT is the most useful predictive factor for ASC.

1. Introduction

Adenosquamous carcinoma of the pancreas (ASC) is a variant of pancreatic ductal adenocarcinoma (PDAC), exhibiting both glandular and squamous differentiation [1–4]. ASC accounts for 3–4% of malignant neoplasms of the pancreas, and is reportedly more aggressive than conventional PDAC, with simultaneous metastases to the liver and lymph nodes being seen more frequently among ASC patients [5,6]. Although diagnosis of ASC is important for predicting the prognosis of patients, recognition of ASC is not easy. One reason for this is that the clinical characteristics of ASC remain unclear because of its rarity. Since most descriptions of ASC have been from case studies and small surgical series [7], its imaging features have not yet been proposed. This study examined the imaging features of ASC in a matched case-control study.

2. Methods

The institutional review board of the hospital approved this study. We evaluated the pathological and clinical records of ASC

* Corresponding author. Department of Gastroenterology, Aichi Cancer Center Hospital, 1-1 Kanokoden, Chikusa-ku, Nagoya, Aichi 464-8681, Japan. Tel.: +81 52 7626111; fax: +81 52 7635233.
E-mail address: hiroshi.imaoka.md@me.com (H. Imaoka).

http://dx.doi.org/10.1016/j.pan.2014.02.005
1424-3903/

and pancreatic neoplasm patients treated at our institution between 2001 and 2012. All cases were diagnosed based on cytological or histological confirmation from surgical specimens or endoscopic ultrasound-guided fine-needle aspiration (EUS-FNA), and only cases in whom imaging data of both contrast-enhanced computed tomography (CT) and endoscopic ultrasonography (EUS) were available were included in this study. The criteria for pathological diagnosis of ASC have been previously described [1,8]. Patients with a history of squamous cell carcinoma or other cancers were excluded from this analysis, to distinguish between primary ASC and metastasis from other sites [9].

Patients were evaluated by EUS using a GF-UCT240 convex array echoendoscope (Olympus Optical Co. Ltd., Tokyo, Japan), and EUS-FNA was performed after EUS examination, as previously described [10,11].

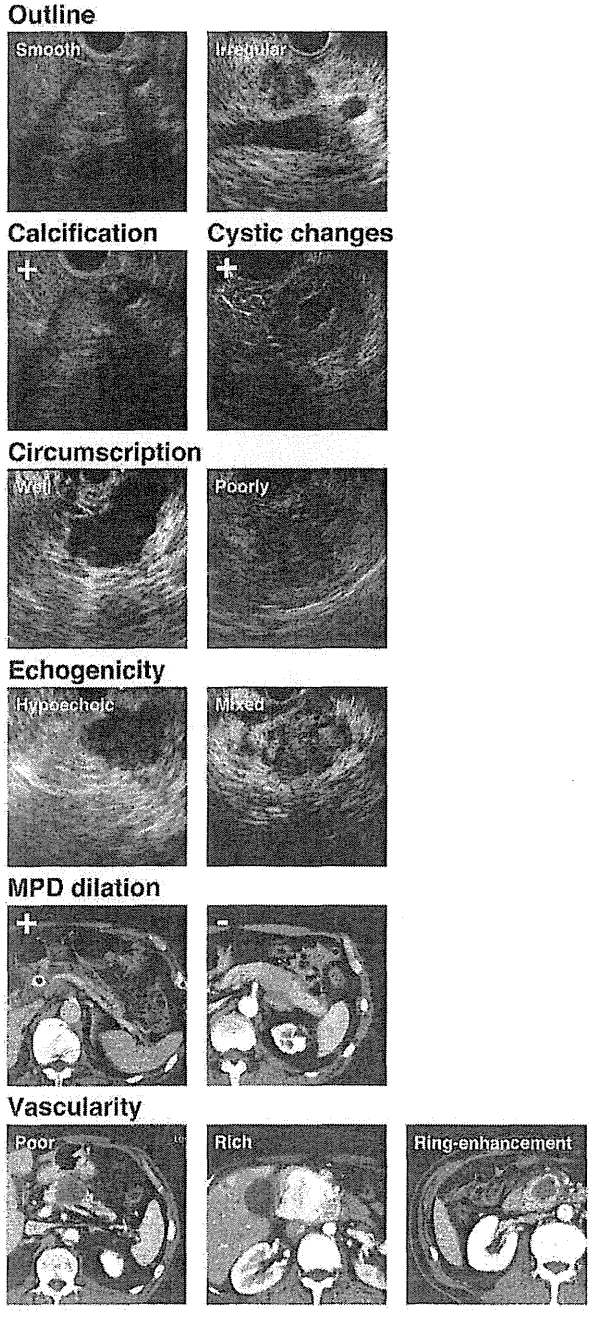

Fig. 1. Representative examples of the imaging parameters.

As controls, cases with solid pancreatic neoplasms, matched in a 2:1 ratio to ASC cases for age (±3 years), sex and tumor location, were also included in this study. Data were abstracted from medical records by 2 reviewers (T.O., T.O.) who were blinded to case-control status. Two reviewers independently assessed these data, and disagreements were resolved by discussion with a third reviewer (K.Y.).

Images of contrast-enhanced CT were reviewed by two blinded radiologists (K.Y., M.K.), and that of EUS were evaluated by two experienced endosonographers (A.S., M.S.). All the evaluators were blind to the patients' pathological and clinical data, which they independently assessed in a random order. Any disagreements were resolved by discussion with a fifth reader (K.Y.). The imaging data were evaluated for the following 7 parameters: outline (smooth vs. irregular), calcification, cystic changes, circumscription (well vs. poorly circumscribed), echogenicity (hyperechoic, hypoechoic and mixed pattern), main pancreatic duct (dilated vs. not dilated), and vascularity (poor, rich and ring-enhancement). We defined the main pancreatic duct as being dilated if it was greater than 2 mm in diameter. In addition, the ring-enhancement pattern was defined as an area of decreased density surrounded by a bright thin rim due to concentration of the contrast-enhancing dye. Representative images are shown in Fig. 1. Five of the 7 parameters (outline, calcification, cystic changes, circumscription and echogenicity) were evaluated on EUS images, while 5 parameters (outline, calcification, cystic changes, main pancreatic duct, and vascularity) were evaluated on contrast-enhanced CT images.

3. Statistical analysis

To compare the patients' backgrounds between ASC and control groups, univariate analysis was performed using the Student's *t*-test for continuous variables, and chi-square test or Fisher's exact test for categorical variables. To compare the various imaging findings between ASC and control groups, univariate analysis was performed using the chi-square test or Fisher's exact test for categorical variables. Multivariate analysis was performed to assess the independent effects of imaging parameters in predicting the diagnosis of ASC using a stepwise forward logistic regression analysis. The likelihood ratio test was used to assess the statistical significance of the variables for the final model. The sensitivity, specificity, positive predictive value (PPV) and negative predictive value (NPV) for diagnosis of ASC were indicated by 95% confidence intervals (CI).

For assessment of interobserver variability of categorical imaging findings, a κ analysis was performed. The levels of agreement were defined as: no agreement ($\kappa < 0$), slight agreement ($\kappa = 0.00$–

Table 1
Baseline characteristics of the patients.

	ASC ($N = 23$)	Control ($N = 46$)	*P*-value
Age (yr)			
	63.26 ± 8.30	62.43 ± 9.06	0.715[a]
Sex			
Male (%)	15 (65.21)	30 (65.21)	
Female (%)	8 (34.78)	16 (34.78)	1.000[b]
Tumor location			
Head (%)	10 (43.47)	20 (43.47)	
Body-Tail (%)	13 (56.52)	26 (56.52)	1.000[b]
Size (mm)	41.26 ± 14.56	36.00 ± 17.54	0.234[a]
CEA (ng/ml)	38.44 ± 85.32	76.10 ± 273.48	0.539[a]
CA19-9 (U/ml)	16,094.10 ± 53,959.46	7931.90 ± 20,165.07	0.485[a]

ASC, adenosquamous carcinoma; yr, years; SD, standard deviation.
[a] Student's *t*-test.
[b] Chi-square test.

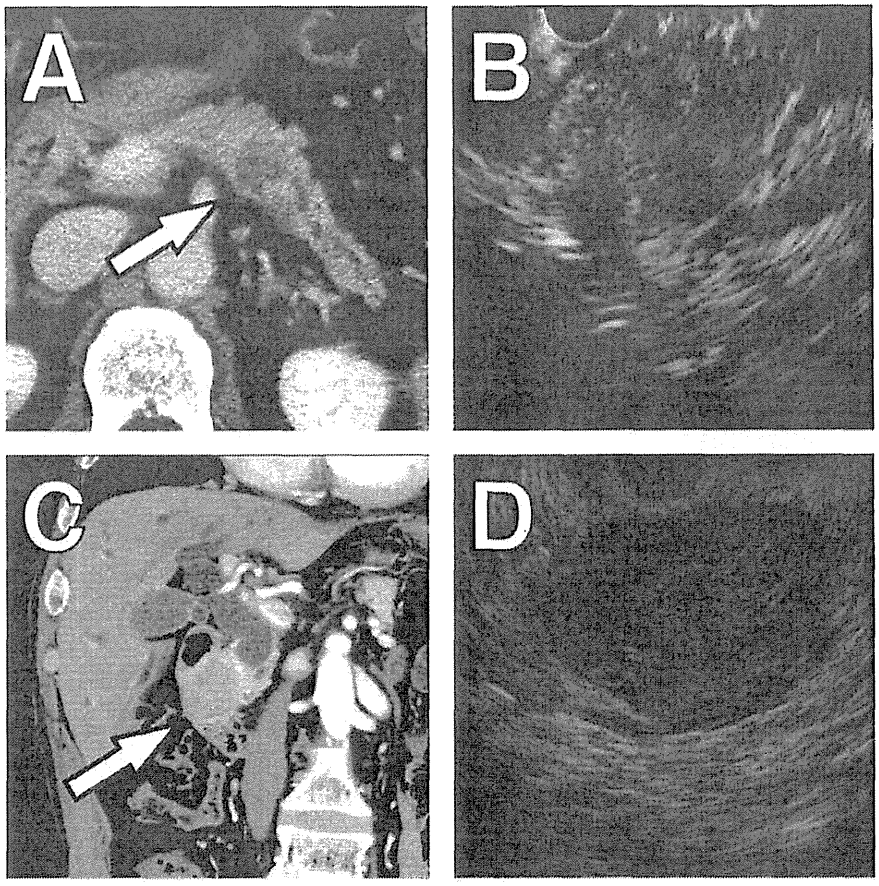

Fig. 2. Representative images of control cases. Pancreatic ductal adenocarcinoma. (A) Contrast-enhanced CT showed a hypodense tumor in the body of the pancreas with pancreatic duct dilatation (white arrow), and (B) EUS showed a mixed-echoic mass with an irregular border. Pancreatic neuroendocrine tumor. (C) Contrast-enhanced CT showed a hyperdense tumor in the head of the pancreas (white arrow), and (D) EUS showed a well-circumscribed hypoechoic mass.

0.20), fair agreement (κ = 0.21–0.40), moderate agreement (κ = 0.41–0.60), substantial agreement (κ = 0.61–0.80), and almost perfect agreement (κ = 0.81–1.00) [12].

All values represent mean ± standard deviation. Values of $P < 0.05$ were considered statistically significant and all P values were two-sided. Data were analyzed using STATA version 11.1 statistical software (StataCorp, College Station, TX, USA).

4. Results

Of the 996 patients with pancreatic neoplasms treated at our hospital between 2001 and 2012, a total of 34 cases of ASC were identified, 23 of who met the inclusion criteria. Of them, 5 patients were diagnosed based on surgical findings, and the others were diagnosed based on EUS-FNA findings. The patients' characteristics are summarized in Table 1. Mean age at diagnosis was 63.26years (range, 44–79 years). Males were affected more frequently than females. Ten of these cases (43.47%) were located in the pancreatic head and the others were in the pancreatic body-tail. The characteristics of the control group in the matched case-control study are also shown in Table 1. Details of the control group were as follows: pancreatic ductal adenocarcinoma (PDAC) in 43 cases, pancreatic neuroendocrine tumor (PNET) in 2 cases and acinar cell carcinoma (ACC) in 1 case. Representative images of control cases (PDAC and PNET) are shown in Fig. 2. Although the tumor size tended to be larger in ASC than in control patients, the difference was not statistically significant.

The differences in the imaging parameters between the two groups are shown in Table 2. Of them, two imaging findings were statistically significantly different between ASC and control groups. A smooth outline of the tumor on contrast-enhanced CT was seen more frequently in ASC than control group patients ($P < 0.001$). Further, vascularity of the tumor on contrast-enhanced CT showed significant differences between ASC and control groups ($P < 0.001$). The ring-enhancement pattern of the tumor tended to be seen more frequently in the ASC than the control group. With regard to interobserver agreement in categorical imaging findings, κ values demonstrated substantial agreement for EUS (0.69) and almost perfect agreement for contrast-enhanced CT (0.90).

The results of stepwise forward logistic regression analysis with the diagnosis of ASC and control as dependent variables and the imaging parameters as independent variables are shown in Table 3. Of them, a smooth outline, cystic changes, and the ring-enhancement pattern on contrast-enhanced CT were identified as significant predictive signs. Further, the likelihood ratio test showed that these 3 parameters were statistically significant in predicting ASC ($P = 0.025$, $P = 0.003$, and $P < 0.001$, respectively). In discriminating ASC from other solid pancreatic neoplasms, the predictive diagnostic sensitivity, specificity, PPV and NPV of a smooth outline on contrast-enhanced CT were 43.5%, 93.5%, 76.9% and 76.8%, respectively, and those of cystic changes on

Table 2
Differences in the imaging parameters between adenosquamous carcinoma and control groups.

		ASC ($N = 23$)	Control ($N = 46$)	P-value
Outline				
CT	Smooth	10	3	
	Irregular	13	43	<0.001[a]
EUS	Smooth	7	5	
	Irregular	16	41	0.088[a]
Calcification				
CT	+	2	2	
	−	21	44	0.596[a]
EUS	+	1	4	
	−	22	42	0.658[a]
Cystic changes				
CT	+	8	9	
	−	15	37	0.167[b]
EUS	+	6	7	
	−	17	39	0.334[a]
Circumscription				
EUS	Well	19	33	
	Poor	4	13	0.323[b]
Echogenicity				
EUS	Hyperechoic	1	1	
	Hypoechoic	10	20	
	Mixed	12	25	0.877[b]
Main pancreatic duct				
CT	Dilated	13	27	
	Not dilated	10	19	0.863[b]
Vascularity				
CT	Poor	8	37	
	Rich	0	4	
	Ring-enhancement	15	5	<0.001[b]

[a] Fisher's exact test.
[b] Chi-square test.

contrast-enhanced CT were 34.8%, 80.4%, 47.1% and 71.2%, respectively. The ring-enhancement pattern was the most useful predictive parameter, and its predictive diagnostic sensitivity, specificity, PPV and NPV were 65.2%, 89.6%, 75.0% and 84.3%, respectively (Table 4).

The surgically resected specimens were soft, fleshy and circumscribed. A representative case is shown in Fig. 3. The tumor was encapsulated by fibrous tissue. Histological assessment of the resected specimen revealed both glandular and squamous differentiation intimately admixed. Neoplastic cells admixed with numerous delicate vessels were present at the margin of the tumor, and extensive tumor necrosis was seen at the center of the tumor. These histological patterns were seen in 80% of the cases.

Table 3
The results of stepwise forward logistic regression analysis of the 7 imaging parameters, to determine their predictive ability for adenosquamous carcinoma.

		Coefficient (β)	95% confidence interval	P-value	Odds ratio
Smooth outline	**CT[a]**	**2.362**	**0.059–4.665**	**0.044**	**10.618**
	EUS	2.361	−0.251–4.974	0.076	10.608
Calcification	CT	0.528	−2.267–3.324	0.711	1.696
	EUS	0.357	−2.606–3.321	0.813	1.429
Cystic changes	**CT[b]**	**2.969**	**0.701–5.238**	**0.010**	**19.488**
	EUS	−2.600	−5.236–0.035	0.053	0.074
Well circumscribed	EUS	−0.988	−3.030–1.053	0.343	0.372
Main pancreatic duct dilatation	CT	1.763	−0.162–3.690	0.073	5.833
Hypoechogenicity	EUS	1.241	−4.586–7.068	0.676	3.460
Mixed echogenicity	EUS	0.459	−5.315–6.234	0.876	1.583
Ring-enhancement	**CT[c]**	**3.862**	**1.504–6.220**	**0.001**	**47.570**

[a] Likelihood-ratio test; P-value; 0.025.
[b] Likelihood-ratio test; P-value; 0.003.
[c] Likelihood-ratio test; P-value; < 0.001.

5. Discussion

ASC is a malignant neoplasm of the pancreas, exhibiting both glandular and squamous differentiation. ASC is considered a variant of PDAC, accounting for 3–4% of malignant neoplasms of the pancreas [2–4]. It is considered to have a poor prognosis due to its aggressive behavior [13–15]. Boyd et al. described in their population-based analysis that overall survival (OS) following surgical resection of ASC is significantly worse as compared to that after resection of PDAC [5]. We also previously clarified that ASC is more aggressive than conventional PDAC in a matched case-control study [6]. In that study, median OS was significantly worse for ASC (8.38 months) than for PDAC (15.75 months; hazard ratio, 1.94), and simultaneous metastases to the liver and lymph nodes were seen more frequently in the ASC group than in the PDAC group. Clinically, diagnosis of ASC is important for predicting the prognosis of patients, although recognition of ASC is not easy. One reason for this is that little is known about the imaging features of ASC because of its rarity. This study, therefore, examined the imaging features of ASC in a matched case-control study.

In the matching process, control cases were carefully selected from among patients with solid pancreatic neoplasms by two blinded reviewers, the cases comprising 43 PDAC patients (93.4%), 2 PNET patients (4.3%), and 1 ACC patient (2.1%). Reportedly, the incidence of PDAC, PNET and ACC is about 90%, 2% and 1–2% of pancreatic neoplasms, respectively [16–19]. Our control group makeup was, thus, consistent with the reported incidence of each type of pancreatic neoplasm. This indicates the adequacy of our matching process.

Two of the imaging parameters, namely tumor outline and ring-enhancement pattern on contrast-enhanced CT, were seen more frequently in ASCs. Furthermore, stepwise forward logistic regression analysis demonstrated that a smooth outline, cystic changes, and the ring-enhancement pattern on contrast-enhanced CT were significant predictive signs of ASC. Pathologically, the tumor was encapsulated by fibrous tissue. Viable neoplastic cells with numerous delicate vessels were present at the margins of the tumor, and prominent necrosis was seen at the center. Thus, a smooth outline, cystic changes, and the ring-enhancement pattern on contrast-enhanced CT may reflect these pathological findings. The ring-enhancement pattern was the most useful imaging parameter, with a predictive diagnostic sensitivity and specificity in discriminating ASC from other solid pancreatic neoplasms of 65.2% and 89.6%, respectively. The diagnostic sensitivity of the ring-enhancement pattern for ASC, on the other hand, was relatively modest. This could be because several cases of ASC resembled conventional PDAC on contrast-enhanced CT images. We speculate that visualization of the pattern may depend on the degree of necrosis within the tumor. On the other hand, the PPV for ASC was 75.0%, which is a satisfactory result. This finding is important, since presence of the ring-enhancement pattern indicates a poor prognosis for patients. Once a diagnosis of ASC is made, newer chemotherapeutic regimens, such as gemcitabine + erlotinib [20] and FOLFIRINOX [21], can be attempted.

In this study, we used a combination of CT and EUS to examine imaging features of ASC using a matched case-control design. Use of this combination seems reasonable since CT and EUS are widely accepted as the most accurate imaging modalities in the diagnosis of pancreatic tumors. In a comparative study of CT and EUS, the sensitivity of CT was reported as 86% and that of EUS was reportedly 98–100% [22,23]. EUS is superior to CT for tumor and nodal staging of pancreatic cancers, while CT can identify distant non-nodal metastases more accurately than EUS [24,25]. Furthermore, the two imaging modalities complement each other during decision-making regarding therapeutic strategies in patients with